JOURNAL OF MATERIALS SCIENCE 17 (1982) 3317–3326

Electrical transport in heavy rare-earth iron garnets

H. B. LAL, B. K. VERMA, VIJAYEE RAM YADAV*
Department of Physics, University of Gorakhpur, Gorakhpur 273001, India

The measurements of electrical conductivity (σ) in the temperature range 450 to 1250 K and thermoelectric power (S) in the temperature range 600 to 1200 K of sintered pressed pellets of rare-earth iron garnets (REIG) with a general chemical formula $RE_3Fe_5O_{12}$ (where RE = Y, Gd, Dy, Ho, Er and Yb) are reported. Values corresponding to the crystalline state have been evaluated employing pore fraction correction. It is observed that plots of log σT against T^{-1} are linear with breaks in the slopes of temperature T_1 (lying between 560 and 578 K) and T_2 ($\sim$ 1000 K). However, plots of S against T^{-1} are linear over the entire temperature range. The results have been discussed using the usual electrical transport theories and it has been concluded that electrical conduction in these solids up to a temperature of 1250 K is extrinsic in which holes localized on Fe^{3+} sites (Fe^{4+} centres created by native defects) conduct via a thermally activated hopping mechanism. Mobility activation energy, mobility and the number of such centres in each garnet are also evaluated.

1. Introduction

Garnet is the name given to a series of compounds with a general chemical formula $M_3T_5O_{12}$, where M stands for lanthanides Sm to Lu and Y while T stands for Fe, Ga, Al, etc. These compounds were first prepared and identified independently by Bertaut and Forrat [1] and Geller [2, 3]. All rare-earth iron garnets (REIG) exhibit typical ferrimagnetic properties [4, 5] and have high initial permeability, low hysteresis loss and high resistivity at room temperature. Owing to these properties, some of them find use in various technical applications [6–8]. In these applications they are used in different forms, e.g. single crystals, thin films and even as polycrystalline materials. Thus the study of magnetic and electrical properties of REIG seems interesting and important. The magnetic properties of REIG have been well studied [4–13]; however, there are only few studies [14–21] regarding their electrical transport behaviour. The only compound which is well studied [13–17] in this respect is YIG (yttruim iron garnet with a chemical formula $Y_3Fe_5O_{12}$). For the last several years our group has been examining the electrical transport in rare-earth compounds such as their oxides [22–24], tungstates [25–27], molybdates [28–30] and orthochromites [31, 32]. Recently, we have studied the electrical transport properties of REIG, particularly heavy rare-earth iron garnets (HREIG) and part of these studies are reported in this paper. All HREIG have a cubic lattice with eight molecules per unit cell. Magnetic ordering in these compounds occurs around 560 K. Some of the physical properties of the garnets studied are given in Table I.

2. Material and experimental techniques

All HREIG were prepared using their respective sesquioxides (RE_2O_3 from Rare-Earth Product Ltd, England, with a stated purity of 99.99%) and Fe_2O_3 (from M/S Bond, India, with a stated purity of 99.99%) in the ratio 3:5 by molecular weight, using the common method reported in the literature [1, 2, 3, 6]. The stoichiometric amount of starting materials were thoroughly mixed, pellet-

*Present address: Department of Physics, S.D. Degree College Math-Lar, Deoria, India.

0022–2461/82/113317–10$03.70/0

ized and heated at 1400° C for 5 h in a platinum crucible in air. These pellets were cooled, crushed, reground to fine powders, made into pellet form again and refired under the same conditions for 10 to 12 h. The final products were characterized by the X-ray diffraction method using Cu$K\alpha$ (λ = 0.15405 nm) radiation.

For measurements of thermoelectric power (S) and electrical conductivity (σ) the prepared REIG powders were pressed in the form of pellets at pressure, P, ranging from 2×10^7 to 12×10^7 kg m^{-2}. The pellets were annealed around 1000° C for 2 days before measurement. No weight loss was noticed after annealing. The pellets used for measurement of S had an area (A) of about 9×10^{-5} m^2 and thickness of 5 to 8 mm. The thermo-e.m.f. (ΔE) was measured using a Keithley digital multimeter type-171 having an internal impedance of 10^{10} Ω. The sample holder used in this measurement is described elsewhere [33]. Thin platinum foils pressed on the faces of the pellets served as electrodes. Sufficient time (~ 1 h) was allowed after applying the temperature gradient (ΔT) before recording the thermo-e.m.f. ΔT was measured using a chromel–alumel thermocouple. The overall reproducibility in the S measurements was about 10%. An altogether different sample holder, described elsewhere [31] was used for the measurement of σ. The d.c. electrical conductivity was determined by measuring current and voltage across the sample using the two-electrode method. The a.c. conductivity at 0.1, 1.0 and 10 kHz was measured using an LCR bridge (Systronic, India: type-921). The overall accuracy in measurement of σ was better than 2% at all temperatures. The details are described elsewhere [21].

3. Results and discussion

Electrodes play an important role in the measurement of σ and S. Roberts [34] has discussed it in detail and have suggested that ohmic contact is the first stringent requirement for such measurements. To ensure ohmic contact between pellet and electrode interface the current through each pellet was measured as a function of applied d.c. voltage at a constant temperature and the results were plotted as J (current density) against E (applied electric field) plots. Two such typical plots for GdIG and YbIG are shown in Fig. 1. Similar plots were obtained for other REIG. The reversal of electric field does not have any effect on these plots. The plots of J against E reveal that J increases linearly with E up to a critical field E_m, after which a change in slope occurs but linear variation continues up to a field of E_0. For field $E > E_0$ the variation of J with E becomes non-linear. Thus contact between electrode and pellet interface remains ohmic between applied field E_m and E_0. The range of E_m and E_0 for different REIG varies from (2.5 to 3.0) $\times$ 10^3 V m^{-1} to (1.0 to 2.0) $\times$ 10^4 V m^{-1}, respectively. In a subsequent study of σ, the applied value of electric field has been chosen to fall within this range. The electrical conductivity value for sintered pellets (σ_p) of REIG does not depend upon the dimensions of the pellets. This indicates that contact resistance between electrode and pellet interface is not very significant and σ_p represents the bulk value of electrical conductivity for the pressed pellet. However, the density (d_p) and σ_p both depend upon P. Both increase initially with P but tend to become constant for pellets made at $P > 6 \times 10^7$ kg m^{-2}. Typical plots for d_p and σ_p against P are shown

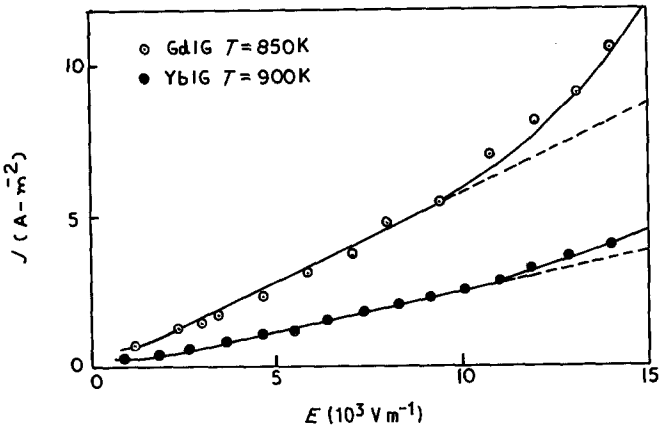

Figure 1 Plots of current density (J) against applied electric field (E) for GdIG and YbIG pellets.

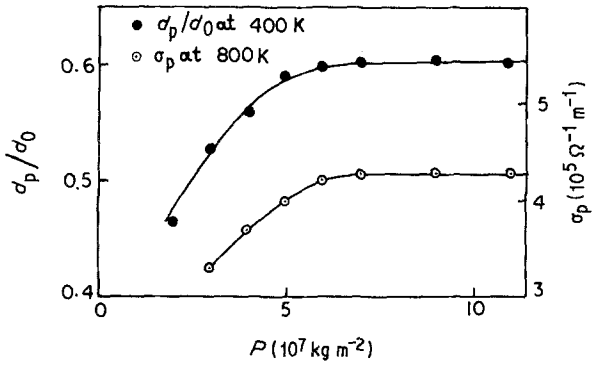

Figure 2 Plots of ratio of pellet density to X-ray density (d_p/d_0) and electrical conductivity of pressed pellets (σ_p) as a function of pelletizing pressure for GdIG.

in Fig. 2. Plots for other REIG are similar. It was observed from these plots that the highest observed value of d_p remains less than the X-ray density (d_0) of the material. This indicates that even highly pressed and sintered pellets contain pores. The values of d_0, d_p and pore fraction ($f = (d_0 - d_p)/d_0$) for pressed pellets of REIG are given in Table I. Therefore, a correction for pore fraction has to be applied to obtain the crystalline value of electrical conductivity. This has been done using the relation [35]:

$$\sigma = \sigma_p[1 + f(1 + f^{2/3})^{-1}]. \quad (1)$$

Equation 1 seems to hold good for $f < 0.4$. S does not show any pressure dependence within the accuracy of our measurement and probably needs no correction for pore fraction. Even after correcting for pore fraction, it is essential to see how significant are the grain-boundary effects. To see this, σ_p was measured as a function of applied signal frequency at constant temperatures for all REIG and typical plots for GdIG are shown in Fig. 3. Similar plots are obtained for other REIG [21]. It has been observed that there is only slight variation of $\sigma_{a.c.}$ at lower temperature, however it remains independent of frequency at higher temperature ($T > 900$ K). This indicates that grain-boundary effects are sufficiently minimized for highly pressed pellets at least at higher temperatures.

The first step in the understanding of electrical transport in any solid is to know whether conductivity is ionic, electronic or mixed (partially ionic and electronic). There are several ways of determining this [36]. The simplest way is to measure $\sigma_{d.c.}$ as a function of time using electrodes which block ionic conduction. In the case of pure ionic conduction, $\sigma_{d.c.}$ decreases with time and tends to become zero after a sufficiently long time; whereas for a pure electronic conductor it is essentially independent of time. For mixed conduction it decreases with time but tends to stabilize at some finite constant value, which is the electronic contribution. To check the type of conduction on the basis of the above logic, $\sigma_{d.c.}$ for all REIG pellets were measured at constant temperature as a function of time using platinum foil electrodes [20, 21]. The typical results for GdIG are shown in Fig. 4. Similar plots are observed for all other REIGs. It was observed that $\sigma_{d.c.}$ decreases with time but becomes almost constant after 20 sec. The ratio of instantaneous, $\sigma_{d.c.(0)}$, to steady state, $\sigma_{d.c.(\infty)}$, electrical conductivity varies from 1.05 to 1.09 for different garnet pellets at different temperatures. This indicates that REIGs are essentially

TABLE I Some physical parameters of garnets studied

Garnets	Lattice constant,* a_0 (nm)	d_0 (10^3 kg m^{-3})	d_p(10^3 kg m^{-3}) at $P = 8 \times 10^7$ kg m^{-2}	Pore fraction	Néel temperature (K)
YIG	1.2376	5.17	3.20	0.38	560
GdIG	1.2471	6.44	3.90	0.39	564
DyIG	1.2405	6.61	3.92	0.40	563
HoIG	1.2375	6.77	4.05	0.40	567
ErIG	1.2347	6.87	4.07	0.40	556
YbIG	1.2302	7.06	4.16	0.41	548

*From Espinosa [44]. *J. Chem. Phys.* 37 (1962) 2344.

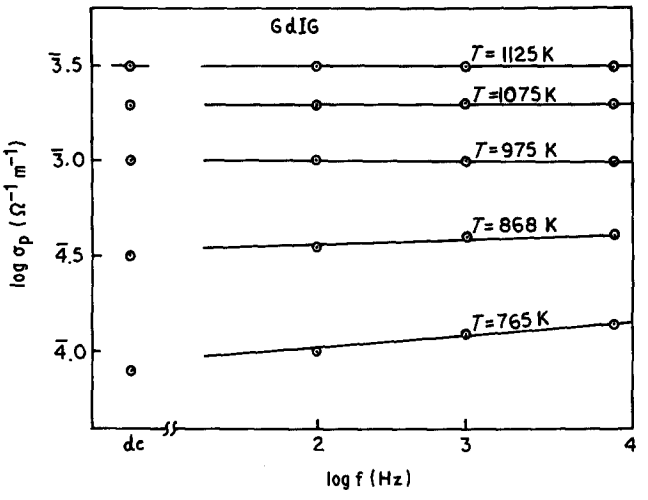

Figure 3 Plot of pellet electrical conductivity (σ_p) versus applied signal frequency ($\log f$) for GdIG at constant temperatures.

electronic conductors and ionic conduction remains less than 9% at all temperatures.

The d.c. electrical conductivity of pellets of each garnet made at $P > 6 \times 10^7$ kg m^{-2} and sintered at 1000° C for 30 h have been measured as a function of temperature (450 to 1250 K). The conductivity values for a particular garnet do not differ much from sample to sample. It is also independent of pellet thickness. Furthermore, for each pellet no significant difference has been observed in conductivity values during the heating and cooling cycles. It is also independent of thermal history and shelf life of the pellet. The mean value of conductivity for a few pellets of each garnet has been taken as the bulk value of conductivity of pressed pellets and from these, crystalline values of electrical conductivity have been calculated using Equation 1. The σ values for a series of REIG lie between 10^{-9} and 10^{-1} Ω^{-1} m^{-1} in the temperature range 450 to 1250 K. Obviously, at room temperature, REIG will be good insulators. The σ variation with temperature for different garnets are presented in Fig. 5 as plots of $\log \sigma T$ against T^{-1}. Close observation of this figure reveals that plots of $\log \sigma T$ against T^{-1} for each REIG can be divided into three parts: part I for $T < T_1$, part II for $T_1 < T < T_2$ and part III for $T > T_2$. These temperatures T_1, and T_2 may be termed break temperatures and are listed in Table II for different REIGs. In each region the plot of $\log \sigma T$ against T^{-1} is linear and can be expressed by the relation

$$\sigma T = \sigma_{0i} \exp -\frac{E_{ai}}{kT} , \qquad (2)$$

where $i = 1$, 2 and 3 represents the first, second and third region of the conductivity plot starting from the lower temperature. The values of the pre-exponential constant (σ_{0i}) and activation energy (E_{ai}) have been evaluated from experimental plots and are given in Table II. It is worth pointing out at this stage that the activation energies listed in Table II are for well-sintered pellets made at higher pressure ($P > 6 \times 10^7$ kg m^{-2}). A change of activation energy by a few percent occurs if measurements are done on freshly prepared unsintered pellets or on pellets made at lower pressure. It is also evident from Fig. 5 that around $T = T_1$, conductivity jumps by a factor of 2 to 5. A maximum jump of five times occurs for GdIG. T_1 for all REIGs lies very close to ferrimagnetic

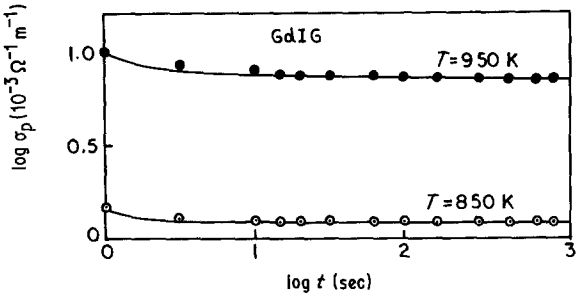

Figure 4 Plots of electrical conductivity (σ_p) of GdIG pellets as a function of log time ($\log t$) at fixed temperatures.

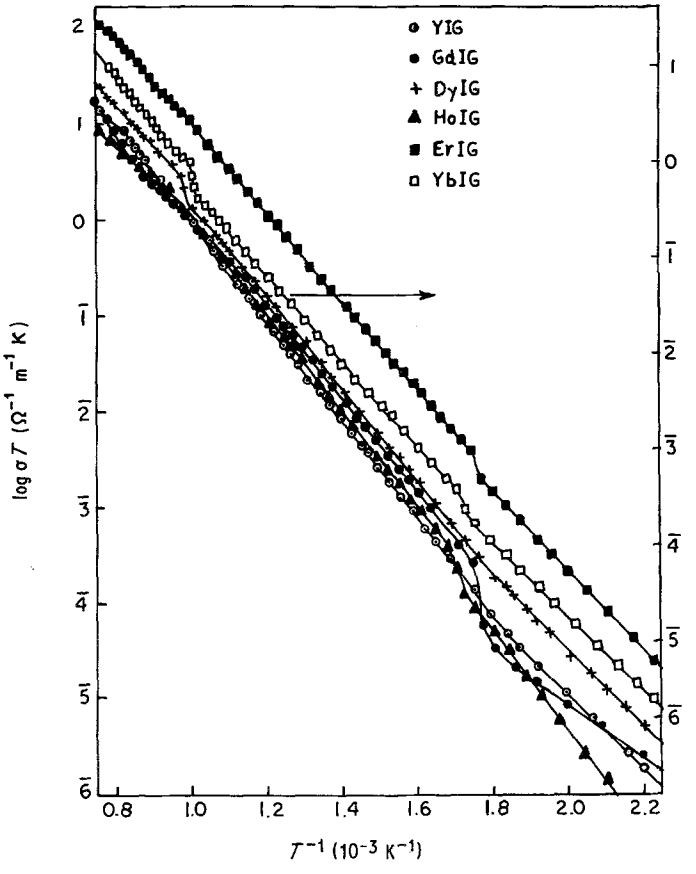

Figure 5 Plots of logarithm of the product of electrical conductivity and temperature (log σT) against inverse of absolute temperature (T^{-1}) for rare-earth iron garnets.

Néel (or Curie) temperature (T_{FN}) (listed in Table I) and this sudden change in σ may be attributed to magnetic disordered scattering. No jump, but only a change in slope in the plots of $\log \sigma T$ against T^{-1} are observed at $T = T_2$ for all garnets except DyIG and YbIG.

The thermoelectric voltage (ΔE) developed across each pellet of the garnet material does not significantly depend upon heating and cooling cycles and repeatable values (within ± 10%) are obtained in successive observations. The results of variations in S at different temperatures (600 to 1200 K) for the REIGs studied are given in Fig. 6 as plots of S against T^{-1}. No break in these plots is observed and the S against T^{-1} curves are linear over the whole range of temperature. Within experimental accuracy the variation of S with T can be represented by the following equation

$$S = \eta(T^{-1}) + H. \qquad (3)$$

The experimental values of η and H for different garnets are given in Table III.

Before presenting analysis of the data it must be made clear that we adopt the so-called standard convention for the sign [37] of S which is opposite to the sign used in the usual text books.

TABLE II Pre-exponential constants (σ_{01}, σ_{02} and σ_{03}), activation energies (E_{a_1}, E_{a_2} and E_{a_3}) and break temperatures (T_1 and T_2) for REIG

Garnets	$T < T_1$		T_1(K)	$T_1 < T < T_2$		T_2(K)	$T > T_2$	
	σ_{01}(Ω^{-1} m^{-1})	E_{a_1}(eV)		σ_{02}(Ω^{-1} m^{-1})	E_{a_2}(eV)		σ_{03}(Ω^{-1} m^{-1})	E_{a_3}(eV)
YIG	1.03×10^3	0.76	562	3.37×10^4	0.90	1000	1.02×10^5	0.96
GdIG	4.96	0.55	560	1.12×10^5	0.94	1000	4.12×10^5	0.88
DyIG	5.10×10^3	0.79	560	2.29×10^5	0.97	1000	3.84×10^5	0.80
HoIG	1.12×10^3	0.80	568	1.69×10^5	0.98	1000	1.66×10^4	0.80
ErIG	9.14×10^4	0.82	562	1.86×10^6	0.98	1000	1.85×10^5	0.84
YbIG	7.93×10^2	0.73	578	1.95×10^5	0.93	1000	1.91×10^5	1.04

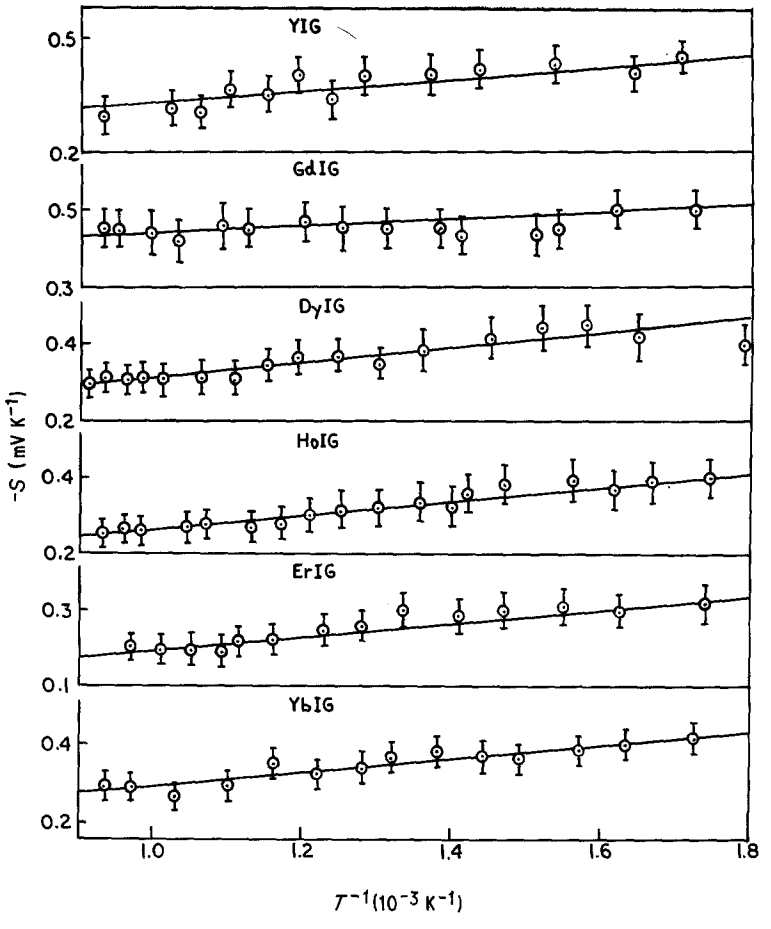

Figure 6 Plot of thermoelectric power (S) against inverse of temperature (T^{-1}) for rare-earth iron garnets.

According to this convention $S = \Delta E/\Delta T$, and has a negative sign for positive charge carrier and *vice versa*. From the time dependence of $\sigma_{d.c.}$ it is clear that REIGs are essentially electronic conductors. Electronic conduction is broadly classified in two types (band or hopping types). It is customary to explain electronic conduction using the energy-band model and we shall first attempt to examine our results using this model. The energy bands which may be relevant in the electrical conduction of rare-earth iron garnets are filled O^{2-}:2p band, RE^{3+}:4f degenerate level (or partially filled narrow band), partially filled Fe^{3+}:3d band, empty Fe^{2+}:3d band, empty Fe^{3+}:4s band, empty RE^{2+}:4f degenerate level (or narrow band) and empty RE^{3+}:5d band. The detailed energy-band calculations are not available for any of the garnets studied. Neither are relevant

TABLE III Summarized thermoelectric power results and values of n, ΔH_m, μ, N_s and theoretical values of S at 800 K

Garnets	η(V) ± 0.05 V	H (mV K^{-1})	n (10^{23} m^{-3})	ΔH_m(eV)	μ at 800 K (10^{-10} m^2 V^{-1} sec^{-1})	N_s (10^{26} m^{-3})	S (mV K^{-1})
YIG	0.10	0.28	6.38	0.80	6.93	4.22	0.34
GdIG	0.12	0.26	5.97	0.82	9.33	4.11	0.34
DyIG	0.16	0.18	8.53	0.81	9.22	4.15	0.31
HoIG	0.17	0.10	6.00	0.81	6.96	4.22	0.34
ErIG	0.17	0.03	43.70	0.81	14.26	4.25	0.28
YbIG	0.17	0.14	1.44	0.76	21.70	4.29	0.35

optical data available for all the garnets studied. This makes it difficult to correctly locate the relative positions of these bands. The only alternative in a such situation is to sketch a qualitative schematic energy-band diagram based on some experimental results for these and other related compounds. For YIG (yttruim iron garnet), where 4f levels are absent, a qualitative energy-band diagram has been sketched on the basis of various experimental results by Larsen and Metsellaar [39]. This energy-band diagram may form a basis for sketching the band diagram for other rare-earth iron garnets. In the case of YIG, the lower edge of the Fe^{3+}:4s band has been found to lie more than 3 eV above the top of the O^{2-}:2p band. However, they have evoked uncertainty regarding the relative position of the filled O^{2-}:2p band and partially filled Fe^{3+}:3d band. We have found by magnetic susceptibility studies [19] that Fe^{4+} ions stabilize in rare-earth iron garnets. This stability of Fe^{4+} gives an indication that in REIG, the Fe^{3+}:3d band lies above the top of the O^{2-}:2p band. From our electrical conductivity measurement on REIG (presented in this paper) it has been found that these are slightly less than that in an Fe_2O_3 ceramic [38] but are much larger than rare-earth sesquioxides (RE_2O_3) [22]. This indicates that RE^{3+} bands are not significant in the electrical conduction of REIG. On the basis of this one can place the bottom of the RE^{3+}:5d band above the top of the Fe^{3+}:4s band. The relative position of the RE^{3+}:$4f^n$ and RE^{2+}:$4f^{n+1}$ levels will depend upon the RE ions concerned. Taking the cases of those RE ions, which are relevant in present study, the position of the RE^{3+}:$4f^n$ level will be lowest in the case of Lu^{3+}:$4f^{14}$ and highest in the case of Tb^{3+}:$4f^8$. The $4f^n$ levels corresponding to other (between Tb and Lu) ions will lie between these levels. However, the Gd^{3+}:$4f^7$ level will be at a higher position compared to Lu^{3+}:$4f^{14}$ but may be at a lower position compared to $4f^n$ levels of the other RE^{3+} ions. The case for the RE^{2+}:$4f^{n+1}$ levels will be similar. However, here the Gd^{2+}:$4f^8$ level will be at the top and the Yb^{2+}:$4f^{14}$ level at the bottom. The relative placement of these levels in the energy-band diagram cannot be indicated with certainty. However, RE^{3+} ions do not affect the conductivity much, and hence those levels may not lie between the O^{2-}:2p and Fe^{3+}:4s band. Caution must be placed when regarding this, and it may not be difficult for some of the levels such as Tb^{3+}:$4f^8$ to lie above the top of the O^{2-}:2p band or Yb^{2+}:$4f^{14}$ to lie below the bottom of Fe^{3+}:4s and above the top of Fe^{2+}:3d bands. However, as we shall see later, their relative position is not very important in the conduction process. Based on the above arguments a general schematic energy-band diagram for rare-earth iron garnets has been drawn as indicated in Fig. 7. It is essential to point out at this point that the effect of the crystal field has not been considered while drawing the energy-band diagram.

In the case of YIG, the energy difference between different bands has been indicated by the analysis of optical studies. It has been found that the difference between the top of the filled O^{2-}:2p band to the bottom of the Fe^{2+}:3d band is more than 3 eV. A difference of similar order between the O^{2-}:2p and Fe^{2+}:3d band has also been observed in the case of rare-earth orthoferrites [38, 40]. Mizushima *et al.* [41] have found a difference of 3 eV between degenerate Fe^{3+}:$3d^5$ levels and Fe^{2+}:$3d^6$ level in Fe-doped TiO_2. All rare-earth garnets are very similar in their structure and behaviour. Therefore, on the basis of the results on YIG and data on related compounds, a difference in energy between the top of O^{2-}:2p to the bottom of the Fe^{2+}:3d band can be assigned to be more than 3 eV.

The striking feature of the energy-band diagram (Fig. 7) is that the partially filled Fe^{3+}:3d band lies above the top of the uppermost completely filled O^{2-}:2p band. Thus on simple band theory, these garnets should show a high-metallic-type conductivity. However, experimentally we have found that pure garnets are insulators at room temperature and do not show metallic conduction even at higher temperature. This means that electrons in the Fe^{3+}:3d bands are localized. This is quite possible due to a correlation effect between electrons. These facts prompt us to conclude that Fe^{3+}:3d bands in garnets are narrow and do not support band conduction. The case for Fe^{2+}:3d, RE^{3+}:4f and RE^{2+}:4f bands may be similar.

Based on our energy-band diagram (Fig. 7), the intrinsic band conduction in rare-earth iron garnets can be suggested to occur by following processes:

(i) electrons are excited from the O^{2-}:2p to the Fe^{3+}:4s band creating holes in the former. The conduction in this process may be dominated by electrons in the latter band;

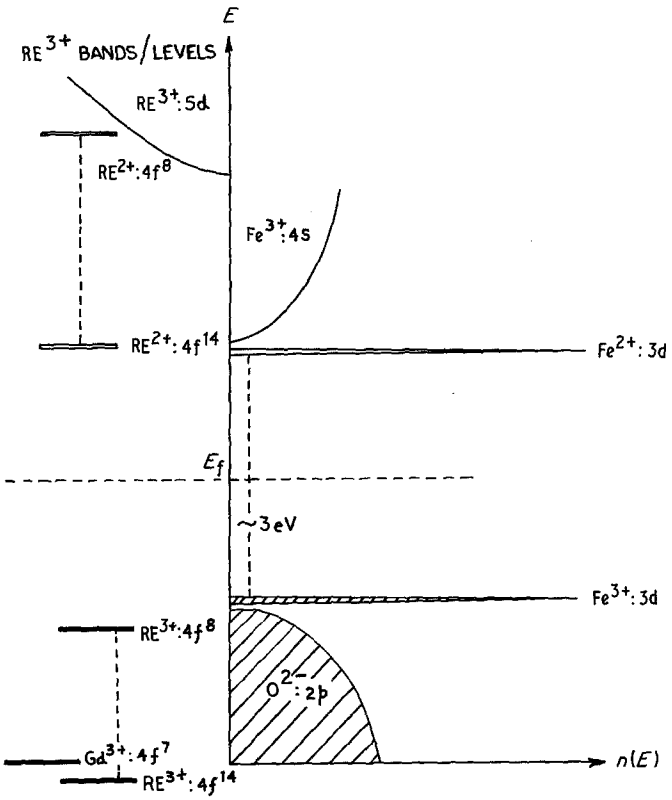

Figure 7 Schematic energy-band scheme for rare-earth iron garnets. Crystal field splitting of bands is not considered.

(ii) electrons are excited from the O^{2-}:2p to the Fe^{2+}:3d band creating holes in the former band. The conduction in this process may be dominated by holes in the oxygen band;

(iii) electrons are excited from the Fe^{3+}:3d band to the Fe^{3+}:4s band creating holes in the d-band. The conduction in this process will be dominated by electrons in the Fe^{3+}:4s band;

(iv) electrons are excited from a filled O^{2-}:2p band to an empty RE^{2+}:$4f^{n+1}$ level creating holes in the O^{2-}:2p band. Holes will be the dominant charge carriers in this process;

(v) besides the above, one can list processes which involve pairs of Fe^{3+}:3d, Fe^{2+}:3d, RE^{3+}:$4f^{n}$ and RE^{2+}:$4f^{n+1}$ levels. However, they have been excluded here as these levels (or narrow bands) may not support band conduction. However, a hopping-type mobility, in which electrons will be the dominant charge carrier, may result if the above-mentioned bands are involved.

Thermoelectric power measurements indicate that in all the garnets studied and over the temperature range studied holes are the dominant charge carrier in electrical conduction. This rules out processes (i), (iii), and (v) suggested above for the electrical conduction. Processes (ii) and (iv), which give holes as the entity of charge carrier, will need an energy of more than 1.5 eV. The maximum activation energy observed in the electrical conduction of these garnets is 1 eV. Furthermore the estimated values of mobility from the pre-exponential factor (σ_0) using the normal relation for a conventional semiconductor (taking $m_e = m_h$ and $\mu_e = \mu_h$) in the higher temperature range are of the order of 10^{-10} m^2 V^{-1} sec^{-1}, which are an order of magnitude less than the mobility one expects in band conduction. On the above considerations even processes (ii) and (iv) listed above are ruled out as being effective in garnets, at least in the temperature range studied.

It is observed from Fig. 6 that S in the temperature range 600 to 1200 K is not very dependent upon temperature. They yield an activation energy of the order of 0.1 eV, against an activation energy of ~1 eV in the case of the plot $\log \sigma T$ against T^{-1}. The difference in activation energy obtained from plots of S against T^{-1} and $\log \sigma T$ against T^{-1} suggest that the mobility of charge carriers is thermally activated. Near constancy of S with T indicates that the number of charge carriers is almost constant. Thus conduction can

be attributed to localized charged impurities. p-type conduction with thermally activated hopping can result owing to the presence of Fe^{4+} centres. The presence of these centres has been supported by our magnetic studies [19]. These centres may result from native defects. This is not strange as conduction in orthoferrites, orthochromites and orthomagnetites is believed to occur by formation of impurity centres Fe^{4+}, Cr^{4+} and Mn^{4+} due to native defects [32, 38].

The electrical conductivity resulting from Fe^{4+} centres in a REIG is given by the expression

$$\sigma T = \frac{ne^2a^2\nu_0}{k} \exp(-E_a/kT), \quad (4)$$

where n is the number of Fe^{4+} centres per unit volume, e is the electronic charge, a is the average distance between Fe^{4+} and Fe^{3+} sites, ν_0 is the hopping frequency that corresponds to the optical phonon frequency, and the other symbols have their usual meanings. The number of Fe^{4+} centres using experimental values of σ and E_a have been evaluated using the above relation and are given in Table III. The thermoelectric power (S) due to charge carriers localized on Fe^{4+} centres is given by the expression [42, 43].

$$S = \frac{k}{e}\left(\frac{S_R^*}{k} - \log\frac{C}{1-C}\right), \quad (5)$$

where S_R^* is the effective entropy of the lattice, which is temperature independent and $C = n/N_S$, where N_S is the total number of available carriers in the state. Usually S_R^*/k is negligibly small and can be omitted. This reduces the above formula to the following relation

$$S = \frac{k}{e}\log\left(\frac{N_S}{n} - 1\right). \quad (6)$$

In the context of rare-earth iron garnets, N_S and n will be the number of Fe^{3+} and Fe^{4+} ions per unit volume, respectively. Using the above relation, S for all garnets has been evaluated and the results are given in Table III together with the values of n and N_S. These values compare well with the average value of S observed for REIG over the entire temperature range.

However, looking at the variation of S with temperature, we notice that it is not exactly constant over the entire temperature range as required by the Equation 6, but has a small temperature dependence. This small temperature dependence indicates that the number of Fe^{4+} centres does not remain constant over the entire temperature range but changes a little with temperature. Taking the above fact into consideration, we can divide the activation energy (E_a) appearing in the conductivity expression into two parts as

$$E_a = \Delta H_m + e\eta, \quad (7)$$

where ΔH_m is the actual enthalpy for charge-carrier hopping and $e\eta$ is the energy appearing in the variation of S with T^{-1} and should be associated with charge-carrier formation. The effective mobility of the charge-carrier hop is then given by the expression

$$\mu = \frac{ea^2\nu_0}{kT} \exp\left(-\frac{\Delta H_m}{kT}\right), \quad (8)$$

where the symbols have their usual meaning. Knowing E_a and η (Tables II and III, respectively) ΔH_m for different garnets has been evaluated using Equation 7. Using these values, μ has been evaluated for different garnets at 800 K and the values are listed in Table III. The order of mobility is quite appropriate for hopping-type conductivity.

Acknowledgements

This work forms a part of a Ph.D. Thesis of one of the authors (V.R.Y.) and was supported by U.G.C., India, through a Teacher Fellowship programme. This financial assistance of U.G.C. is gratefully acknowledged.

References

1. F. BERTAUT and F. FORRAT, *Compt. Rend. Acad. Sci. Paris* **242** (1956), 382.
2. S. GELLER and M. A. GILLEO, *Acta. Cryst.* **10** (1957) 239.
3. *Idem, J. Phys. Chem. Solids* **3** (1957) 30.
4. R. PAUTHNET, *Compt. Rend. Acad. Sci. Paris* **242** (1956) 1859; **243** (1956) 1499.
5. F. PERTAUT and R. PAUTHNET, *Proc. Inst. Elect. Eng. Part B Suppl.* **104** (1957) 261.
6. R. W. COPPER, W. A. CROSALEY, J. L. PAGE and R. F. PEARSON, *J. Appl. Phys. (USA)* **39** (1968) 555.
7. R. S. TEBBLE and P. J. CRAIK, "Magnetic Materials" (John Wiley, London, 1969).
8. K. J. STANDLEY, "Oxide Magnetic Materials" (Clarendon Press, Oxford, 1972).
9. F. F. Y. WANG, *Treat. Mater. Sci. Technol.* **2** (1973) 279.
10. R. ALENARD and J. C. BARBIER, *J. Phys. Rad.* **20** (1959) 378.
11. S. GELLER, H. J. WILLIAMS and R. C. SHERWOOD, *Phys. Rev.* **123** (1961) 1692.

12. R. F. PEARSON, *J. Appl. Phys. (USA)* **33** (1962) 1236.
13. C. D. BRANDLE and S. BLANK, *IEEE Trans. Mag. Mag.* **12** (1976) 14.
14. E. E. ANDERSON, *J. Appl. Phys. (USA) Suppl.* **30** (1959) 299.
15. D. ELWELL and A. DIXON, *Solid State Commun.* **6** (1968) 585.
16. R. E. FOUNTANA and D. J. EPSTEEN, *Mat. Res. Bull. (USA)* **6** (1971) 959.
17. Ya. M. KSENDZOV, A. M. KOTEN NIKOVA and V. V. MARKOV, *Sov. Phys. Solid State (USA)* **15** (1974) 1563.
18. P. K. LARSEN and R. METSELAAR, *Phys. Rev.* **B14** (1976) 2520.
19. V. R. YADAVA and H. B. LAL, *Jap. J. Appl. Phys.* **18** (1979) 2229.
20. *Idem, Canad. J. Phys.* **57** (1979) 1204.
21. V. R. YADAVA, PhD thesis, Gorakhpur University, Gorakhpur, India (1980).
22. H. B. LAL, B. K. VERMA and N. DAR, *Ind. J. Cryogenic* **1** (1976) 119.
23. H. B. LAL, V. PRATAP and A. KUMAR, *Pramana* **9** (1978) 409.
24. H. B. LAL, *J. Phys. C. Solid State Phys.* **13** (1980) 3969 and our other references therein.
25. N. DAR and H. B. LAL, *Mat. Res. Bull (USA)* **14** (1979) 1263.
26. B. K. VERMA, Ph.D. thesis, Gorakhpur University, Gorakhpur, India (1979).
27. H. B. LAL, *J. Mag. Mag. Mat. (USA)* **23** (1981), 41, and our other references therein.
28. R. N. PANDEY, V. PRATAP and H. B. LAL, *Proc. Nat. Acad. Sci. (India)* **48A** (I) (1978) 1.
29. A. K. TRIPATHI and H. B. LAL, *Jap. J. Appl. Phys.* **49** (1980) 1896.
30. H. B. LAL and V. PRATAP, *J. Mater. Sci.* **16** (1981) 377, and our other references given therein.
31. A. K. TRIPATHI and H. B. LAL, *Mat. Res. Bull. (USA)* **15** (1980) 233.
32. A. K. TRIPATHI, PhD thesis, Gorakhpur University, Gorakhpur, India (1981).
33. K. SHAHI, H. B. LAL and S. CHANDRA, *Ind. J. Pure Appl. Phys.* **13** (1975) 1.
34. G. G. ROBERTS, in "Transfer and storage of Energy by Molecules", Vol. 4 (John Wiley, New York, 1974).
35. H. W. RUSSEL, *J. Amer. Ceram. Soc.* **18** (1935) 1.
36. L. HEYNE, "Electrochemistry of Mixed Ionic Electronic Conductors in Solid Electrolytes", edited by S. Geller (Springer-Verlag, New York, 1977) p. 169.
37. S. M. GRIVIN, *J. Solid State Chem.* **25** (1978) 65.
38. G. V. SUBBARAO, B. M. WANKLYN and C. N. R. RAO, *J. Phys. Chem. Solids* **32** (1971) 340.
39. P. K. LARSEN and R. METSELAAR, *J. Solid State Chem.* **12** (1975) 253.
40. J. B. GOODENOUGH, *J. Appl. Phys. (USA)* **37** (1966) 1415.
41. K. MIZUSHIMA, M. TANAKA, A. ASAI, S. IIDA and J. B. GOODENOUGH, *J. Phys. Chem. Solids* **40** (1979) 1129.
42. R. R. HEIKES, "Thermoelectricity: Science and Engineering", edited by R. R. Heikes and R. W. Ure (Interscience, New York, 1961) p. 45.
43. J. B. WEBB, M. SAYER and A. MAN SINGH, *Canad. J. Phys.* **55** (1977) 1725.
44. G. P. ESPINOSA, *J. Chem. Phys.* **37** (1962) 2344.

Received 22 January
and accepted 8 May 1982